



1 **Feedback effects of boundary-layer meteorological**
2 **factors on explosive growth of PM_{2.5} during winter heavy**
3 **pollution episodes in Beijing from 2013 to 2016**

4 Juntong Zhong¹, Xiaoye Zhang^{1, 2}, Yunsheng Dong³, Yaqiang Wang¹, Jizhi Wang¹,
5 Yangmei Zhang¹, Haochi Che⁴

6 ¹State Key Laboratory of Severe Weather & Key Laboratory of Atmospheric Chemistry of CMA,
7 Chinese Academy of Meteorological Sciences, China.

8 ²Center for Excellence in Regional Atmospheric Environment, IUE, Chinese Academy of Sciences,
9 China.

10 ³Key Laboratory of Environmental Optics and Technology, Anhui Institute of Optics and Fine Mechanics,
11 Chinese Academy of Sciences, China.

12 ⁴Department of Physics, University of Oxford, UK.

13 *Correspondence to:* X.Y. Zhang (xiaoye@camsma.cn); Y.S. Dong (ysdong@aiofm.ac.cn)

14 **Abstract.** In January of 2013, February of 2014, December of 2015, and December of 2016 to January
15 10th of 2017, 12 persistent heavy aerosol pollution episodes (HPEs) occurred in Beijing, which has
16 attracted special attention from the public. During the HPEs, the precise cause of explosive growth in
17 fine particulate matter (PM) is uncertain. Here, we analyzed and estimated relative contributions of
18 boundary-layer meteorological factors to such growth, using ground and vertical meteorological data.
19 Beijing HPEs are generally characterized by the transport stage (TS), whose aerosol pollution formation
20 is primarily caused by pollutants transported from the south of Beijing, and the cumulative stage (CS),
21 in which the cumulative explosive growth (PM mass concentration doubled in ~10 hours) is dominated
22 by stable atmospheric stratification characteristic of southerly slight or calm winds, near-ground
23 anomalous inversion, and moisture accumulation. During the CSs, observed southerly weak winds
24 facilitate local pollutant accumulation by limiting the invasion of northerly clean winds and minimizing
25 horizontal pollutant diffusion. Established from TSs, elevated PM levels scatter more solar radiation back
26 to the space to reduce near-ground temperature. This radiation reduction decreases near-ground
27 saturation vapor pressure and very likely causes anomalous inversion. The decreased saturation pressure
28 significantly increases relative humidity; the inversion subsequently reduces vertical turbulent diffusion
29 and boundary layer height to trap pollutants and accumulate water vapor. Appreciable near-ground
30 moisture accumulation (RH>80%) further enhances aerosol hygroscopic growth and accelerates liquid-



31 phase and heterogeneous reactions, in which incompletely quantified chemical mechanisms need more
32 investigation. Noted meteorological feedback on PM explains over 70% in cumulative explosive growth
33 of PM.

34

35 **Keyword:** Southerly transport; anomalous inversion; moisture accumulation; meteorological feedback.

36



37 1 Introduction

38 Since a persistent heavy fog and haze event occurred in eastern China in January 2013, fine
39 particulate matter smaller than 2.5 μm in diameter ($\text{PM}_{2.5}$), as a key component of pollution episodes,
40 has drawn wide attention all over China. Elevated $\text{PM}_{2.5}$ leads a sharp decrease in visibility that affects
41 economic activities by causing traffic disruptions and contains toxic substances that affect respiratory
42 and circulatory system (Chen et al., 2013; Bai et al., 2007). The interaction between aerosol and radiation
43 directly and indirectly affects weather and climate (Zhang et al., 2013; Zhang et al., 2015b; Wei et al.,
44 2011; Boucher et al., 2013; Wang et al., 2010). China has experienced heavy aerosol pollution episodes
45 recently, with $\text{PM}_{2.5}$ reaching unprecedentedly high levels in many cities, particularly Beijing and its
46 vicinity (BIV), which is one of the nation's most polluted regions (Zhang et al., 2012).

47 To elucidate the causes of such heavy pollution episodes, a variety of explanations have been
48 proposed (Huang et al., 2014; Sun et al., 2014a; Sun et al., 2014b; Wang et al., 2014b; Wang et al.,
49 2014c). Previous studies found that atmospheric conditions represented one critical parameter in
50 regulating the cycles of pollution episodes in Beijing in autumn 2013 (Guo et al., 2014; Zhang et al., 2009)
51 and in the North China Plain and other areas in China (Zhang et al., 2015c). During one pollution episode,
52 an analysis of atmospheric background fields revealed dynamic and thermodynamic effects substantially
53 affected pollution formation (Zhang et al., 2014). Specifically, aerosol pollution in Beijing was possibly
54 contributed by southerly/southwesterly surface wind (Wang et al., 2013b). This likely attribution was
55 further verified by source apportionment from the Beijing Environmental Protection Bureau in
56 2012–2013. In addition, aerosol pollution can be formed by secondary aerosol formation through
57 atmospheric chemical reactions, including liquid-phase reactions, in which aqueous SO_2 is oxidized by
58 NO_2 , H_2O_2 and O_3 to form sulfate, and heterogeneous reactions, in which NO_2 and N_2O_5 form nitrates
59 with water (Zheng et al., 2015a; Cheng et al., 2016).

60 Although these cited studies existed, the formation mechanism during different stages for heavy
61 aerosol pollution in Beijing, especially the explosive growth stage of $\text{PM}_{2.5}$ mass concentration, is still
62 not clear. Previous studies focused more on whether unfamiliar chemical mechanisms were not or
63 inadequately considered in Beijing, a region with high concentrations of various aerosol components



64 (Wang et al., 2014b). This view was questioned by subsequent research, suggesting that such rapid
65 growth is mainly attributable to the regional transport of clean and polluted air mass, which derived from
66 the comparison between surface meteorological factors and the PM_{2.5} mass concentration in several cities
67 of the North China Plain (Zheng et al., 2015b). However, the attribution of such growth's drivers is
68 unreasonable occasionally, because the rapid growth may occur with weak surface winds and stable
69 stratification, which are unfavorable for transport. Then vertical meteorological variations in the
70 boundary layer (BL) in one autumnal episode have been analyzed, which significantly affect the PM_{2.5}
71 mass concentration near the ground (Hua et al., 2016). However, in the absence of long-term observations
72 of meteorological factors and pollutant concentrations, most research concerning pollution causes
73 focuses on one or several consecutive pollution episodes in a certain time, and almost no research attempt
74 to investigate, conclude and quantify the contributions of meteorological factors to the majority of heavy
75 pollution episodes since 2013, particularly the feedback effect of meteorological factors during explosive
76 growth processes. Such investigations will definitely provide a clearer understanding of roles that various
77 vertical meteorological factors play in heavy pollution episodes. Therefore, this paper primarily uses
78 vertical measurements of meteorological factors in the BL from 2013 to 2016, investigates their
79 contributions to the explosive growth of PM_{2.5} during the heavy pollution episodes in Beijing, and also
80 attempts to quantify the effect of meteorological factors on the explosive growth of PM_{2.5} levels.
81



82 **2 Methods**

83 In this study, the following data are used. (1) Hourly PM_{2.5} mass concentration measured by national
84 monitoring stations of the Ministry of Environmental Protection. PM_{2.5} mass concentrations of urban
85 stations were averaged to represent urban pollution conditions. (2) Atmospheric vertical observations
86 twice daily at 0800 h and 2000 h, including winds, temperature and relative humidity (RH), measured
87 using L-band radiosonde radar at the observatory (54511) in southern Beijing from 1 January 2013 to 31
88 January 2013, 1 February 2014 to 28 February 2014, 26 November 2015 to 31 December 2015 and 21
89 December 2016 to 10 January 2017. (3) A parameterized index, PLAM (Parameter Linking Aerosol
90 Pollution and Meteorological Elements), calculated with the observations from the observatory (54511),
91 based on the calculation method presented in detail in previous studies (Wang et al., 2013a; Zhang et al.,
92 2015c; Zhang et al., 2009; Wang et al., 2012). (4) Hourly ground-level meteorological observations from
93 automatic weather stations (AWSs) provided by the National Meteorological Information Center of the
94 China Meteorological Administration. (5) Lidar observations were measured by one Mie-elastic
95 backscatter polarization lidar emitting short pulses of 20 Hz at 532nm in the Institute of Atmospheric
96 Physics (116.38E, 39.98N), located in the northern urban area of Beijing. The optical parameters of the
97 aerosol particles were retrieved by the backscattering signals. Then the vertical profiles of the aerosol
98 extinction coefficient and linear depolarization ratio were obtained based on the assumptive lidar ratios
99 as 50 for aerosols using the Fernald's method (Fernald, 1984; Lv et al., 2017).

100

101



102 **3 Results and discussion:**

103 **3.1 Characteristics of explosive growth in HPEs**

104 A period during which the $PM_{2.5}$ level is less than $35 \mu\text{g m}^{-3}$ is defined as a clean period based on
105 the $PM_{2.5}$ daily mean mass concentration limit in the primary standard of China's national environmental
106 quality standards, while a pollution episode is referred to as an episode during which the $PM_{2.5}$ exceeds
107 $80 \mu\text{g m}^{-3}$ for 3 consecutive days between two clean periods. Pollution episodes with peak $PM_{2.5}$ values
108 less than $300 \mu\text{g m}^{-3}$ or more than $400 \mu\text{g m}^{-3}$ are termed light pollution episodes (LPEs) or heavy
109 pollution episodes (HPEs), respectively. During HPEs, the growth processes in which the $PM_{2.5}$ mass
110 concentration increases from less than $30 \mu\text{g m}^{-3}$ to $150\text{--}300 \mu\text{g m}^{-3}$ in the initial several or ten hours or
111 increases by over $150 \mu\text{g m}^{-3}$ rapidly afterward are termed explosive growth processes.

112 Based on the urban $PM_{2.5}$ monthly mean mass concentration in winter Beijing from 2013 to 2016,
113 the months with highest mass concentration each year were selected to represent the severe $PM_{2.5}$
114 pollution conditions in winter, which are January in 2013, February in 2014, December in 2015 and
115 December in 2016 respectively. These months are termed the wintertime pollution period (WPP) for the
116 convenience of further investigation.

117 During the WPP, 12 HPEs occur in total (Figure 1–4 (dark gray)), whose $PM_{2.5}$ mass concentration
118 is $244.3 \mu\text{g m}^{-3}$ on average. The maximum mean value ($307.4 \mu\text{g m}^{-3}$) appears in HPE₁, which has been
119 analyzed in detail in a variety of papers (Zhang et al., 2013; Zhang et al., 2014). The concentrations of
120 HPE₆ and HPE₁₀ are $304.2 \mu\text{g m}^{-3}$ and $294.5 \mu\text{g m}^{-3}$ respectively, which are slightly lower than HPE₁.
121 The minimum mean concentration of $PM_{2.5}$ occurs in HPE₈ ($160.4 \mu\text{g m}^{-3}$), which is nearly twice as much
122 as the mean annual mass concentration of $PM_{2.5}$ in 2015, nevertheless.

123 Typical explosive growth processes (color-mark) in HPEs were selected, which appeared in 11 of
124 the 12 HPEs. The green-mark explosive growth processes are tentatively referred to as transport
125 explosive growth processes, because they generally occur consistently with relatively strong southerly
126 winds compared with subsequent explosive growth and vary sensitively and rapidly in response to wind
127 shift from northerly to southerly in the BL. The red-mark explosive growth processes are tentatively



128 termed cumulative explosive growth processes because of anomalous inversion facilitating pollutant
129 accumulation. The purple-mark explosive growth processes are tentatively known as convergent
130 explosive growth processes, for local wind convergence occurs (Figure 6) with weak wind velocity and
131 no anomalous inversion. The early stages of HPEs during which transport explosive growth occurs are
132 defined as transport stages (TSs), while the later stages during which cumulative/convergent explosive
133 growth appears are termed cumulative stages (CSs).

134 **3.2 Meteorological causes of the explosive growth in HPEs**

135 **3.2.1 PM_{2.5} pollution formation is primarily caused by pollutants transported from the south of** 136 **Beijing, which subsequently worsen weather conditions**

137 We found that during clean periods occur mostly strong northwesterly winds whose velocity
138 increases with height; during the HPEs, the southwesterly winds with dramatically decreased velocity
139 were most frequent (Figure 1-4 (a, b)). Strong northerly winds and weak southerly winds closely
140 correspond to the clean periods and the HPEs respectively, because northwesterly winds, which are from
141 less populated north mountainous areas, carry unpolluted air masses while southerly winds carry polluted
142 air masses from more populated and polluted southern industrial regions (Jia et al., 2008; Liu et al.,
143 2013; Guo et al., 2014).

144 During the TSs with southerly winds, air temperature and moisture substantially increase compared
145 with clean periods with northerly winds (Figure 1-4 (b, c, d)), which indicates warm and humid southerly
146 airflow transport more water vapor and heat into Beijing. During 15 transport explosive growth processes
147 ((green lines)), nearly no striking near-ground (<250m) moisture accumulation appears; no anomalous
148 inversion appears except brief weak inversion, which suggest that vertical variations of temperature and
149 RH are unlike to primarily cause transport explosive growth. Nevertheless, weak inversion and more
150 near-ground moisture favor growth.

151 If we assume that the primary cause of this explosive growth is pollution accumulation due to local
152 emissions, the growth needs to coincide with light ($0.3\sim 1.5\text{ m s}^{-1}$) or calm ($0\sim 0.2\text{ m s}^{-1}$) air observed
153 during the later TSs instead of slight ($1.6\sim 3.3\text{ m s}^{-1}$) or gentle ($3.4\sim 5.4\text{ m s}^{-1}$) breeze observed during the



154 early TSs, because weaker winds result in a stagnant condition, which are more favorable for local
155 accumulation. However, the majority of later TSs with calm air do not exhibit such explosive growth
156 (Figure 1-4 (a, b)), which suggests local emissions under weak winds are likely conducive but not
157 dominant with respect to growth.

158 Before transport explosive growth during HPE₁₋₂, the urban PM_{2.5} mass concentration of Baoding
159 (light gray lines), which is typically representative of pollution conditions in the south of Beijing, was
160 much higher than Beijing; the winds in Beijing rapidly shifted from northerly to southerly. Then the
161 transport explosive growth (green lines) occurred, consistently with southerly slight or gentle breezes in
162 the BL (green boxes). The southerly air mass move more than 288 km d⁻¹ below 500 m (estimated from
163 the measured wind speed), which are fast enough to transport pollutants to Beijing. Similar conditions
164 appeared in 8 of other 9 HPEs with transport explosive growth. Such processes indicate southerly
165 pollutant transport is primarily responsible for the explosive growth, given the pollution transport
166 pathway of the southwest wind belt determined by the unique geographic features of the North China
167 Plain, with the Tai-hang Mountains and the Yan Mountains limiting the invasion of northerly cold air and
168 leading northeast movement of southerly winds. (Su et al., 2004). Governed by this transport pathway,
169 PM_{2.5} mass concentration increased by ~400 µg m⁻³ from less than 35 µg m⁻³ in ten hours on 22 January
170 2013, when winds shifted from northerly to southerly with much higher PM_{2.5} concentrations in Baoding.

171 Pollutants transported from the south of Beijing primarily results in PM_{2.5} pollution formation in the
172 urban Beijing area, to which possible weak inversion and the near-surface moisture accumulation is
173 conducive. Warm and humid airflow from the south transports more water vapor and pollutants to the
174 North China Plain, which creates the requisite moisture and pollution accumulation conditions for
175 subsequently cumulative explosive growth.

176 **3.2.2 Worsening meteorological conditions primarily cause cumulative explosive growth**

177 *Feedback of anomalous inversion on pollutant accumulation*

178 Anomalous inversion occurs during 10 of 12 HPEs (Figure 1~4 (a, c)). The factors that cause
179 inversion in Beijing includes topography, advection and radiation. With the Tai-hang Mountains and the



180 Yan Mountains lying north of Beijing, a cold air mass flows down into the urban of Beijing from the
181 mountain peaks, which occasionally causes topography inversion; advection inversion occurs when a
182 warm and less dense air mass moves over a cold and dense air mass. However, during most cumulative
183 stages, the anomalous inversion appears with slight or calm winds, which suggests that the movement of
184 air masses is not striking, so the contribution of topography and advection to such inversion is limited.
185 The ground exceeds long-wave radiation at night to reduce near-ground temperature to facilitate
186 inversion occasionally. However, almost no anomalous inversion occurs without pre-existing high PM_{2.5}
187 mass concentration in the WPP (Figure 1~4), which suggests that the ground radiation are likely
188 conducive to weak/normal inversion, but not dominant with respect to anomalous inversion.

189 Noted anomalous inversion is preceded by existing relatively high PM_{2.5} levels generally established
190 by the transport explosive growth. Before the cumulative explosive growth, existing aerosols are
191 concentrated below 500 m (Figure 5). These low-layer aerosols back-scatter amounts of radiation to
192 space (Wang et al., 2014a; Gao et al., 2015), and cause a significant reduction in radiation reaching the
193 ground, which further reduces near-ground temperature. These findings indicate that anomalous
194 inversion is primarily due to radiation cooling effect of pre-existing aerosols. Below the inversion, near-
195 ground temperature reduction cools down plumes or thermals of originally warm surface air to decrease
196 thermal turbulence; observed weakened vertical shear of horizontal winds ((F1~4 (b))) produces less
197 vorticity to reduce mechanical turbulence, which further strengthens the existing inversion.

198 Anomalous inversion traps pollution-laden air beneath it due to its strong static stability (Wallace
199 and Hobbs, 2006). It facilitates pollutant accumulation by suppressing vertical air mixing and reducing
200 BL height. During the cumulative explosive growth with anomalous inversion in the HPE₁₀, the turbulent
201 diffusion coefficient rapidly decreases from 100 m² s⁻¹ to 50 m² s⁻¹ (model output of CUACE/Chem, the
202 meso-scale China Meteorological Administration (CMA) Unified Atmospheric Chemistry modelling
203 system, personal communication with Dr. Hong Wang); the BL height decreases from ~500 m in the early
204 morning, to ~350 m at noon, even to ~250 m at night (Figure 5), which coincide with the increase of
205 PM_{2.5} from ~200 to ~450 µg m⁻³ (Figure 4 (a)). The striking layered structure in the BL occurs at the
206 height of ~300 m on 20 December 2016 (Figure 5), which is consistent with the lower edge of anomalous
207 inversion (Figure 4), which verifies the strong inhibition of anomalous inversion. Additionally, a short



208 cold air mass invades the northern urban area of Beijing in the early morning on 20 December 2016. The
209 enhanced movement increases the BL height and reduce the PM_{2.5} mass concentration in part of northern
210 urban area (Figure 5), which slightly reduces the urban mean mass concentration of PM_{2.5} (Figure 4 (1)).
211 However, the anomalous inversion rapidly restore its original structure to facilitate pollutant
212 accumulation.

213 The occurrence of anomalous inversion in 9 HPEs coincides with cumulative explosive growth of
214 PM_{2.5} levels (F1~4 (a, c)), which verifies the suppression of anomalous inversion to pollutants. Note that
215 no cumulative explosive growth of PM_{2.5} levels appears in HPE₃ despite anomalous inversion, partly
216 because the height of the lowest inversion layer in HPE₃ (~750 m) is much higher than that in the 9 HPEs
217 (~ 250 meters), which suggests near-ground inversion is more favorable for pollutant accumulation.

218 *Anomalous inversion results in near-surface moisture accumulation*

219 During clean periods, the moisture is evenly distributed in the BL with RH less than 40%, while
220 during the HPEs, RH is over 60% (even 80%) in the lower or upper BL (Figure 1~4 (c, d)). During the
221 HPEs, in the absence of temperature inversion, moisture vertically distributes in the BL, and the RH in
222 the upper BL is occasionally higher than that of the near-ground surface; in the presence of weak
223 inversion, the lower edge of the inversion layer is in approximate agreement with the RH contour of 60%;
224 In the presence of anomalous inversion (red boxes in Figure 1~4 (c)) in the BL, the lower edge of the
225 strong inversion layer frequently coincides with an RH contour of 80% (red boxes in Figure 1~4 (d)),
226 which is observed in most cumulative explosive growth processes.

227 The previously noted relation of vertical temperature and RH indicates that anomalous inversion
228 results in appreciable near-surface moisture accumulation by suppressing the vertical mixing of the water
229 vapor (Wallace and Hobbs, 2006). The vertical diffusion of the near-surface water vapor as the anomalous
230 inversion disappeared on 1 December 2016, 26 December 2016, and 5 January 2017 verifies the cited
231 research outcome. Noted that mentioned near-ground temperature reduction caused by cooling effects of
232 aerosols is also conducive to moisture accumulation by decreasing near-ground saturation vapor pressure
233 to increase RH.



234 *Moisture accumulation facilitates aerosol hygroscopic growth and additional secondary aerosol*
235 *formation*

236 Strong absorbent aerosol particles absorb and grow, when additional water vapor appears in the air
237 (Zhang et al., 2015a). The mass concentrations of soluble organic aerosols, sulfate, nitrate, and
238 ammonium rapidly increase with RH (Figure S1). After moisture absorption in North China, aerosol
239 particle size increases 20%–60% (Pan et al., 2009) and aerosol direct radiative forcing increases ~50%
240 (Zhang et al., 2015a). As a key component of atmospheric aerosols, aerosol water serves as a medium
241 that enables aqueous-phase reactions (Pilinis et al., 1989; Seinfeld and Pandis, 1986; Ervens et al., 2011).
242 For example, aerosol water serves as a reactor in which alkaline aerosol components trap SO₂, which is
243 then oxidized by NO₂ to form sulfate in northern China (Cheng et al., 2016). The ratio of SO₂ to SO₄²⁻
244 ranges from less than 0.1 at relative humidity (RH) <20% to 1.1 at RH >90%, exhibiting an exponential
245 increase with RH (Wang et al., 2016). In addition, high RH facilitates heterogeneous chemical processes
246 to aggravate air pollution (Zhu et al., 2011). For example, the net reaction probability of HNO₃ uptake
247 on CaCO₃ particles was found to increase with relative humidity from ~0.003 at 10% to 0.21 at 80% (Y.
248 Liu et al., 2008).

249 *Stable atmospheric stratification characteristic of southerly light or calm winds, anomalous inversion,*
250 *and near-ground (<250 m) moisture accumulation (RH>80%) dominates the cumulative explosive*
251 *growth of PM_{2.5}.*

252 During the HPEs, nearly all 10 cumulative explosive growth processes (Figure 1-4) occur
253 concurrently with stable atmospheric stratification primarily characterized by southerly light or calm
254 winds, near-ground anomalous inversion, and cumulative moisture (RH>80%). The weak southerly
255 winds increased with height are conducive to the growth, because relatively strong southerly winds in
256 the upper BL (~1000m) transport pollutants from the south of Beijing, while low-level (~250m) southerly
257 light or calm winds limiting the invasion of northerly cold winds facilitates local pollution accumulation
258 by minimizing horizontal pollutant diffusion. The anomalous inversion facilitates vertical pollutant
259 accumulation by suppressing convection activities. During the cumulative growth process in HPE₁₀, the



260 turbulent diffusion coefficient rapidly decreases from 100 to 50 and the BL height decreases from 500 m
261 to ~250 m, which is extremely favorable for pollutants accumulation. Additional suppression of vertical
262 mixing of water by inversion and previously noted decreased saturation vapor pressure cause near-
263 surface moisture accumulation ($RH > 80\%$). This accumulated moisture facilitates secondary aerosol
264 formation in liquid-phase and heterogeneous reactions to increase $PM_{2.5}$ levels.

265 It's likely that merely weak southerly winds or near-ground anomalous inversion primarily can
266 cause cumulative explosive growth. However, the growth does not occur in the polluted process from 4
267 to 15 December 2015 with weak southerly winds, which indicates that weak southerly winds do not
268 suffice to cause cumulative explosive growth in the absence of anomalous inversion; even with
269 anomalous inversion, no explosive growth appeared on 14 and 24 January 2013, which suggests that
270 anomalous inversion cannot cause explosive growth without weak southerly winds. Therefore,
271 cumulative explosive growth in CSs is primarily resulted from the joint effects of southerly light or calm
272 winds, near-ground anomalous inversion and moisture accumulation.

273 Note that the cumulative explosive growth at 2000 h on 3 January was accompanied by a southerly
274 gentle breeze ($3.4\sim 5.4\text{ m s}^{-1}$), which suggests that low-level southerly pollutant transport occasionally
275 exerts an important impact on the growth, with anomalous inversion and near-ground moisture
276 accumulation.

277 *Feedback of cumulative pollutants on worsening meteorological conditions*

278 Established from cumulative explosive growth, exceedingly high $PM_{2.5}$ levels further decrease the
279 near-ground temperature by reflecting and scattering more solar radiation, which strengthens the existing
280 anomalous inversion and subsequently results in additional pollutant accumulation until the next synoptic
281 process occurs. The near-surface temperature decreased from 3°C at 2000 h on 19 December to -3°C at
282 0800 h on 20 December after elevated ground $PM_{2.5}$ levels (Figure 4 (d)). Then it had remained at $\sim 1^{\circ}\text{C}$
283 with $PM_{2.5}$ of more than $400\text{ }\mu\text{g m}^{-3}$ over the next 2 d until northerly strong and clean winds blew the
284 pollution away on 22 December. Similar processes also occurred in the CSs of other HPEs, which verifies
285 the outcome.



286 3.2.3 Local air convergence is favorable for convergent explosive growth.

287 The explosive growth of $PM_{2.5}$ appears in HPE₄₋₅ without inversion and near-ground moisture
288 accumulation (Figure 2), which suggests previously noted stable atmospheric stratification does not
289 primarily cause the growth. Weak winds in convergent explosive growth processes, particularly the
290 process in HPE₅, eliminate the likely contributions of southerly transport pollution. A comparison of
291 surface wind distributions in the North China Plain before (Figure 6 (a, d)) and during (Figure 6 (b, c; d,
292 e)) the convergent explosive growth processes in HPE₄₋₅ shows that the urban area of Beijing is
293 dominated by northerly winds before the growth, while is characterized by local air convergence during
294 the processes, which suggests that the persistent local convergence is conducive to the explosive growth
295 by causing pollutants to further locally accumulate. The convergent explosive growth in HPE₆₋₇ with air
296 convergence (Figure S2) also verifies the outcome.

297 3.3 Quantification of meteorological contributions to $PM_{2.5}$ cumulative explosive growth

298 Cooling effects of elevated $PM_{2.5}$ levels established from TSs worsen meteorological conditions, which
299 primarily causes cumulative explosive growth. To approximately quantify this atmospheric feedback on
300 the growth, PLAM (Parameter Linking Aerosol Pollution and Meteorological Elements) was used, which
301 was derived from the relationship of $PM_{2.5}$ with key meteorological parameters. The PLAM index, whose
302 details of calculation have been described in Wang et al. (Wang et al., 2013a; Wang et al., 2012), primarily
303 reflects the stability of the air mass and the condensation rate of water vapor on aerosol particles. It has
304 been employed to identify the contribution of specific meteorological factors to a 10 d haze–fog event in
305 2013 (Zhang et al., 2013) and to evaluate the contribution of meteorological factors to changes in
306 atmospheric composition and optical properties over Beijing during the 2008 Olympic Games (Zhang et
307 al., 2009). During cumulative explosive growth processes, the hourly variation of urban mean $PM_{2.5}$ mass
308 concentration is in closely linear agreement with that of PLAM for Beijing (Figure 7 (a–d)). The squared
309 correlation coefficients between PLAM and $PM_{2.5}$ from 2013 to 2016 are 0.71, 0.76, 0.69, and 0.71
310 respectively, exceeding the 0.05 significance level. The mean value of four coefficients is 0.72, which
311 suggests the noted feedback of worsening meteorological conditions on PM explains over 70% in



312 cumulative explosive growth of PM_{2.5}.

313 4 Conclusion:

314 We have characterized different stages of 12 HPEs during the WPP (wintertime pollution periods)
315 in Beijing and typical explosive growth of PM_{2.5} during different stages, including transport, cumulative,
316 and convergent explosive growth. Meteorological causes to such growth are elucidated, based on
317 observations of vertical meteorological factors within the BL (Figure 8). Beijing HPEs can generally be
318 divided into the TS, whose explosive growth is primarily caused by pollutants transported from south of
319 Beijing, and the CS, in which stable atmospheric stratification dominates the cumulative explosive
320 growth of PM_{2.5}.

321 Polluted and humid airflow from the south of Beijing transports water vapor and pollutants to
322 Beijing, which primarily causes transport explosive growth and creates the requisite moisture and
323 pollution accumulation conditions for CSs. Elevated PM_{2.5} levels established from the TS reduce near-
324 ground temperature by back scattering short wave solar radiation. This temperature reduction very likely
325 results in anomalous inversion, which is enhanced by the reduced mechanical turbulence that results from
326 less vorticity caused by observed weakened vertical shear of horizontal winds in the lower BL during the
327 later TSs and decreased thermal turbulence with cooling plumes or thermals of originally warm surface
328 air that result from the decreased near-ground temperature. Anomalous inversion reduces turbulent
329 diffusion and decreases the BL height to trap pollutants. The similar suppression of anomalous inversion
330 to vertical mixing of water vapor and decreased saturation water vapor pressure caused by noted
331 temperature reduction result in appreciable near-surface moisture accumulation (RH>80%). The
332 accumulated moisture facilitates pollutant accumulation by enhancing hygroscopic growth and
333 accelerating liquid-phase and heterogeneous reactions. However, specific reaction mechanisms have not
334 been fully quantified and require additional investigation, particularly their contributions to the explosive
335 growth and the maintenance of PM_{2.5} during CSs. Note that observed southerly weak winds facilitate
336 local pollutant accumulation by limiting the invasion of northerly clean winds and minimizing horizontal
337 pollutant diffusion. The joint effects of southerly weak winds, near-ground anomalous inversion, and
338 moisture accumulation dominate cumulative explosive growth of PM_{2.5}. Nearly 72% of the growth is



339 attributable to noted meteorological feedback, based on correlation analysis between PM_{2.5} and PLAM
340 index during cumulative explosive growth processes. Note that sporadic local air convergence also
341 causes pollutants to further accumulate.

342 Established from cumulative explosive growth, exceedingly high PM_{2.5} levels further decrease the
343 near-ground temperature to strengthen the existing anomalous inversion, which results in additional
344 pollutant accumulation until the next synoptic process occurs.

345 **References**

- 346 Bai, N., Khazaei, M., van Eeden, S. F., and Laher, I.: The pharmacology of particulate matter air
347 pollution-induced cardiovascular dysfunction, *Pharmacology & Therapeutics*, 113, 16, 2007.
- 348 Boucher, O., Randall, D., Artaxo, P., Bretherton, C., Feingold, G., Forster, P., Kerminen, V. V. M., Kondo,
349 Y., Liao, H., Lohmann, U., Rasch, P., Satheesh, S. K., Sherwood, S., Stevens, B., and Zhang, X. Y.:
350 Clouds and Aerosols, in: *Climate Change 2013: The Physical Science Basis. Contribution of Working*
351 *Group I to the Fifth Assessment Report of the Intergovernmental Panel on Climate Change*, edited by:
352 Stocker, T. F., Qin, D., Plattner, G.-K., Tignor, M., Allen, S. K., Boschung, J., Nauels, A., Xia, Y., Bex,
353 V., and Midgley, P. M., Cambridge University Press, Cambridge, United Kingdom and New York, NY,
354 USA, 571-658, 2013.
- 355 Chen, Y., Ebenstein, A., Greenstone, M., and Li, H.: Evidence on the impact of sustained exposure to air
356 pollution on life expectancy from China's Huai River policy, *Proceedings of the National Academy of*
357 *Sciences of the United States of America*, 110, 12936-12941, 10.1073/pnas.1300018110, 2013.
- 358 Cheng, Y., Zheng, G., Chao, W., Mu, Q., Bo, Z., Wang, Z., Meng, G., Qiang, Z., He, K., and Carmichael,
359 G.: Reactive nitrogen chemistry in aerosol water as a source of sulfate during haze events in China,
360 *Science Advances*, 2, 2016.
- 361 Ervens, B., Turpin, B. J., and Weber, R. J.: Secondary organic aerosol formation in cloud droplets and
362 aqueous particles (aqSOA): a review of laboratory, field and model studies, *Atmospheric Chemistry and*
363 *Physics*, 11, 11069-11102, 10.5194/acp-11-11069-2011, 2011.
- 364 Fernald, F. G.: Analysis of atmospheric lidar observations: some comments, *Applied Optics*, 23, 652,
365 1984.
- 366 Gao, Y., Zhang, M., Liu, Z., Wang, L., Wang, P., Xia, X., Tao, M., and Zhu, L.: Modeling the feedback
367 between aerosol and meteorological variables in the atmospheric boundary layer during a severe fog–
368 haze event over the North China Plain, *Atmospheric Chemistry and Physics*, 15, 4279-4295,
369 10.5194/acp-15-4279-2015, 2015.
- 370 Guo, S., Hu, M., Zamora, M. L., Peng, J. F., Shang, D. J., Zheng, J., Du, Z. F., Wu, Z., Shao, M., Zeng,
371 L. M., Molina, M. J., and Zhang, R. Y.: Elucidating severe urban haze formation in China, *Proceedings*
372 *of the National Academy of Sciences of the United States of America*, 111, 17373-17378,
373 10.1073/pnas.1419604111, 2014.
- 374 Hua, Y., Wang, S., Wang, J., Jiang, J., Zhang, T., Song, Y., Kang, L., Zhou, W., Cai, R., Wu, D., Fan, S.,



- 375 Wang, T., Tang, X., Wei, Q., Sun, F., and Xiao, Z.: Investigating the impact of regional transport on
376 PM_{2.5} formation using vertical observation during APEC 2014 Summit in Beijing, *Atmospheric*
377 *Chemistry and Physics*, 16, 15451-15460, 10.5194/acp-16-15451-2016, 2016.
- 378 Huang, R.-J., Zhang, Y., Bozzetti, C., Ho, K.-F., Cao, J.-J., Han, Y., Daellenbach, K. R., Slowik, J. G.,
379 Platt, S. M., and Canonaco, F.: High secondary aerosol contribution to particulate pollution during haze
380 events in China, *Nature*, 514, 218-222, 2014.
- 381 Jia, Y., Rahn, K. A., He, K., Wen, T., and Wang, Y.: A novel technique for quantifying the regional
382 component of urban aerosol solely from its sawtooth cycles, *Journal of Geophysical Research*
383 *Atmospheres*, 113, 6089-6098, 2008.
- 384 Liu, X. G., Li, J., Qu, Y., Han, T., Hou, L., Gu, J., Chen, C., Yang, Y., Liu, X., and Yang, T.: Formation
385 and evolution mechanism of regional haze: a case study in the megacity Beijing, China, *Atmospheric*
386 *Chemistry & Physics*, 13, 4501-4514, 2013.
- 387 Lv, L., Liu, W., Zhang, T., Chen, Z., Dong, Y., Fan, G., Xiang, Y., Yao, Y., Yang, N., and Chu, B.:
388 Observations of particle extinction, PM_{2.5} mass concentration profile and flux in north China based on
389 mobile lidar technique, *Atmospheric Environment*, 2017.
- 390 Pan, X. L., Yan, P., Tang, J., Ma, J. Z., Wang, Z. F., Gbaguidi, A., and Sun, Y. L.: Observational study of
391 influence of aerosol hygroscopic growth on scattering coefficient over rural area near Beijing mega-city,
392 *Atmospheric Chemistry & Physics*, 9, 7519-7530, 2009.
- 393 Pilinis, C., Seinfeld, J. H., and Grosjean, D.: Water content of atmospheric aerosols, *Atmospheric*
394 *Environment*, 23, 1601-1606, 1989.
- 395 Seinfeld, J. H., and Pandis, S. N.: *Atmospheric Chemistry and Physics: From Air Pollution to Climate*
396 *Change*, John Wiley & Sons, USA, 1986.
- 397 Su, F., Gao, Q., Zhang, Z., REN, Z.-h., and YANG, X.-x.: Transport pathways of pollutants from outside
398 in atmosphere boundary layer, *Research of Environmental Sciences*, 1, 26-29, 2004.
- 399 Sun, Y., Jiang, Q., Wang, Z., Fu, P., Li, J., Yang, T., and Yin, Y.: Investigation of the sources and evolution
400 processes of severe haze pollution in Beijing in January 2013, *Journal of Geophysical Research:*
401 *Atmospheres*, 119, 4380-4398, 2014a.
- 402 Sun, Y. L., Jiang, Q., Wang, Z. F., Fu, P. Q., Li, J., Yang, T., and Yin, Y.: Investigation of the sources and
403 evolution processes of severe haze pollution in Beijing in January 2013, *J. Geophys. Res.-Atmos.*, 119,
404 4380-4398, 10.1002/2014jd021641, 2014b.
- 405 Wallace, J. M., and Hobbs, P. V.: *Atmospheric science : an introductory survey*, Elsevier, 2006.
- 406 Wang, G., Zhang, R., Gomez, M. E., Yang, L., Levy Zamora, M., Hu, M., Lin, Y., Peng, J., Guo, S.,
407 Meng, J., Li, J., Cheng, C., Hu, T., Ren, Y., Wang, Y., Gao, J., Cao, J., An, Z., Zhou, W., Li, G., Wang, J.,
408 Tian, P., Marrero-Ortiz, W., Secretst, J., Du, Z., Zheng, J., Shang, D., Zeng, L., Shao, M., Wang, W.,
409 Huang, Y., Wang, Y., Zhu, Y., Li, Y., Hu, J., Pan, B., Cai, L., Cheng, Y., Ji, Y., Zhang, F., Rosenfeld, D.,
410 Liss, P. S., Duce, R. A., Kolb, C. E., and Molina, M. J.: Persistent sulfate formation from London Fog to
411 Chinese haze, *Proc Natl Acad Sci U S A*, 113, 13630-13635, 10.1073/pnas.1616540113, 2016.
- 412 Wang, H., Zhang, X., Gong, S., Chen, Y., Shi, G., and Li, W.: Radiative feedback of dust aerosols on the
413 East Asian dust storms, *Journal of Geophysical Research*, 115, 6696-6705, 2010.
- 414 Wang, J., Wang, Y., Liu, H., Yang, Y., Zhang, X., Li, Y., Zhang, Y., and Deng, G.: Diagnostic identification
415 of the impact of meteorological conditions on PM_{2.5} concentrations in Beijing, *Atmospheric*
416 *Environment*, 81, 158-165, 10.1016/j.atmosenv.2013.08.033, 2013a.



- 417 Wang, J., Wang, S., Jiang, J., Ding, A., Zheng, M., Zhao, B., Wong, D. C., Zhou, W., Zheng, G., Wang,
418 L., Pleim, J. E., and Hao, J.: Impact of aerosol–meteorology interactions on fine particle pollution during
419 China’s severe haze episode in January 2013, *Environmental Research Letters*, 9, 094002, 10.1088/1748-
420 9326/9/9/094002, 2014a.
- 421 Wang, J. Z., Gong, S., Zhang, X. Y., Yang, Y. Q., Hou, Q., Zhou, C., and Wang, Y.: A parameterized
422 method for air-quality diagnosis and its applications, *Advance of Meteorology*, doi:10.1155/2012/238589,
423 1-10, 2012.
- 424 Wang, X., Chen, J., Sun, J., Li, W., Yang, L., Wen, L., Wang, W., Wang, X., Collett, J. L., and Shi, Y.:
425 Severe haze episodes and seriously polluted fog water in Ji’nan, China, *Sci. Total Environ.*, 493, 133-137,
426 2014b.
- 427 Wang, Z., Li, J., Wang, Z., Yang, W., Tang, X., Ge, B., Yan, P., Zhu, L., Chen, X., and Chen, H.: Modeling
428 study of regional severe hazes over mid-eastern China in January 2013 and its implications on pollution
429 prevention and control, *Science China Earth Sciences*, 57, 3-13, 2014c.
- 430 Wang, Z. B., Hu, M., Wu, Z. J., Yue, D. L., He, L. Y., Huang, X. F., Liu, X. G., and Wiedensohler, A.:
431 Long-term measurements of particle number size distributions and the relationships with air mass history
432 and source apportionment in the summer of Beijing, *Atmospheric Chemistry and Physics*, 13, 10159-
433 10170, 10.5194/acp-13-10159-2013, 2013b.
- 434 Wei, P., Cheng, S. Y., Li, J. B., and Su, F. Q.: Impact of boundary-layer anticyclonic weather system on
435 regional air quality, *Atmospheric Environment*, 45, 2453-2463, 10.1016/j.atmosenv.2011.01.045, 2011.
- 436 Y. Liu, E.R. Gibson, J.P. Cain, H. Wang, V.H. Grassian, ‡ and, and A. Laskin: Kinetics of Heterogeneous
437 Reaction of CaCO₃ Particles with Gaseous HNO₃ over a Wide Range of Humidity, *Journal of Physical
438 Chemistry A*, 112, 1561, 2008.
- 439 Zhang, L., Sun, J. Y., Shen, X. J., Zhang, Y. M., Che, H., Ma, Q. L., Zhang, Y. W., Zhang, X. Y., and
440 Ogren, J. A.: Observations of relative humidity effects on aerosol light scattering in the Yangtze River
441 Delta of China, *Atmospheric Chemistry & Physics*, 15, 2853-2904, 2015a.
- 442 Zhang, R. H., Li, Q., and Zhang, R. N.: Meteorological conditions for the persistent severe fog and haze
443 event over eastern China in January 2013, *Science China Earth Sciences*, 57, 26-35, 2014.
- 444 Zhang, R. Y., Wang, G. H., Guo, S., Zarnora, M. L., Ying, Q., Lin, Y., Wang, W. G., Hu, M., and Wang,
445 Y.: Formation of Urban Fine Particulate Matter, *Chemical Reviews*, 115, 3803-3855,
446 10.1021/acs.chemrev.5b00067, 2015b.
- 447 Zhang, X., Sun, J., Wang, Y., Li, W., Zhang, Q., Wang, W., Quan, J., Cao, G., Wang, J., Yang, Y., and
448 Zhang, Y.: Factors contributing to haze and fog in China, *Chinese Science Bulletin (Chinese Version)*,
449 58, 1178, 10.1360/972013-150, 2013.
- 450 Zhang, X. Y., Wang, Y. Q., Lin, W. L., Zhang, Y. M., Zhang, X. C., Gong, S., Zhao, P., Yang, Y. Q., Wang,
451 J. Z., and Hou, Q.: Changes of Atmospheric Composition and Optical Properties Over BEIJING—2008
452 Olympic Monitoring Campaign, *Bulletin of the American Meteorological Society*, 90, 1633–1651, 2009.
- 453 Zhang, X. Y., Wang, Y. Q., Niu, T., Zhang, X. C., Gong, S. L., Zhang, Y. M., and Sun, J. Y.: Atmospheric
454 aerosol compositions in China: spatial/temporal variability, chemical signature, regional haze distribution
455 and comparisons with global aerosols, *Atmos. Chem. Phys.*, 11, 26571-26615, 2012.
- 456 Zhang, X. Y., Wang, J. Z., Wang, Y. Q., Liu, H. L., Sun, J. Y., and Zhang, Y. M.: Changes in chemical
457 components of aerosol particles in different haze regions in China from 2006 to 2013 and contribution
458 of meteorological factors, *Atmos. Chem. Phys.*, 15, 12935-12952, 10.5194/acp-15-12935-2015, 2015c.



459 Zheng, B., Zhang, Q., Zhang, Y., He, K. B., Wang, K., Zheng, G. J., Duan, F. K., Ma, Y. L., and Kimoto,
460 T.: Heterogeneous chemistry: a mechanism missing in current models to explain secondary inorganic
461 aerosol formation during the January 2013 haze episode in North China, *Atmospheric Chemistry and*
462 *Physics*, 15, 2031-2049, 10.5194/acp-15-2031-2015, 2015a.

463 Zheng, G. J., Duan, F. K., Su, H., Ma, Y. L., Cheng, Y., Zheng, B., Zhang, Q., Huang, T., Kimoto, T.,
464 Chang, D., Poschl, U., Cheng, Y. F., and He, K. B.: Exploring the severe winter haze in Beijing: the
465 impact of synoptic weather, regional transport and heterogeneous reactions, *Atmospheric Chemistry and*
466 *Physics*, 15, 2969-2983, 10.5194/acp-15-2969-2015, 2015b.

467 Zhu, T., Shang, J., and Zhao, D. F.: The roles of heterogeneous chemical processes in the formation of
468 an air pollution complex and gray haze, *Science China Chemistry*, 54, 145-153, 2011.

469

470



471 **Data Availability**

472 The data that support the findings of this study are available from the corresponding author upon
473 reasonable request.

474

475 **Acknowledgements:**

476 This research is supported by the National Key Project of MOST (2016YFC0203306), and the Basic
477 Scientific Research Progress of the Chinese Academy of Meteorological Sciences (2016Z001).

478

479 **Author Contributions:**

480 X.Y.Z. and Y.Q.W. designed the research; X.Y.Z, J.T.Z and H.C.C carried out the analysis of observations.

481 Y.S.D provided and analyzed laser radar data. Y.M.Z provided aerosol species data. J.Z.W provided

482 PLAM data. J.T.Z. wrote the first manuscript and X.Y.Z. revised the manuscript. All authors read and

483 approved the final version.

484

485 **Additional Information:**

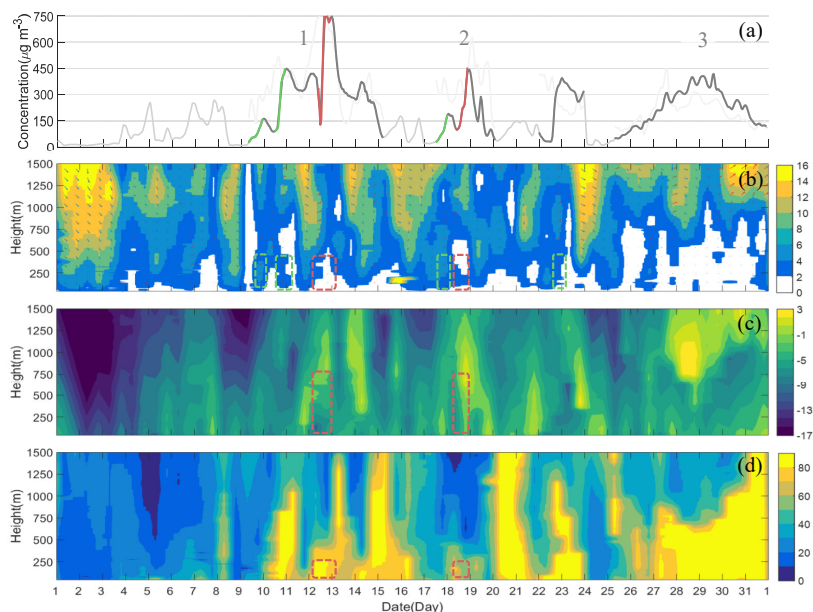
486 **Competing financial interests:** The authors declare no competing financial interests.

487



488 **Figures**

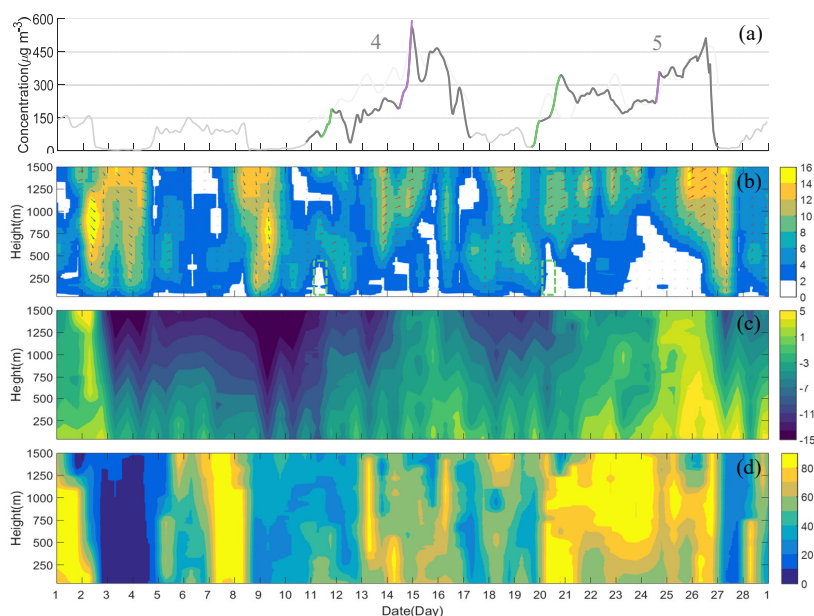
489



490

491 **Figure 1. Temporal variations in urban mean PM_{2.5} and vertical distributions of meteorological factors in**
492 **January 2013.** (a)PM_{2.5} mass concentration (dark gray or gray: Beijing; light gray: Baoding); (b) winds (vectors;
493 red vectors: southwesterly winds) and wind velocity (shadings; units: m/s); (c)temperature (shadings; units:°C);
494 (d)RH (shadings; units: %); (green boxes: transport explosive stages; red boxes: cumulative explosive stages)

495



496

497 **Figure 2. Temporal variations in urban mean PM_{2.5} and vertical distributions of meteorological factors in**

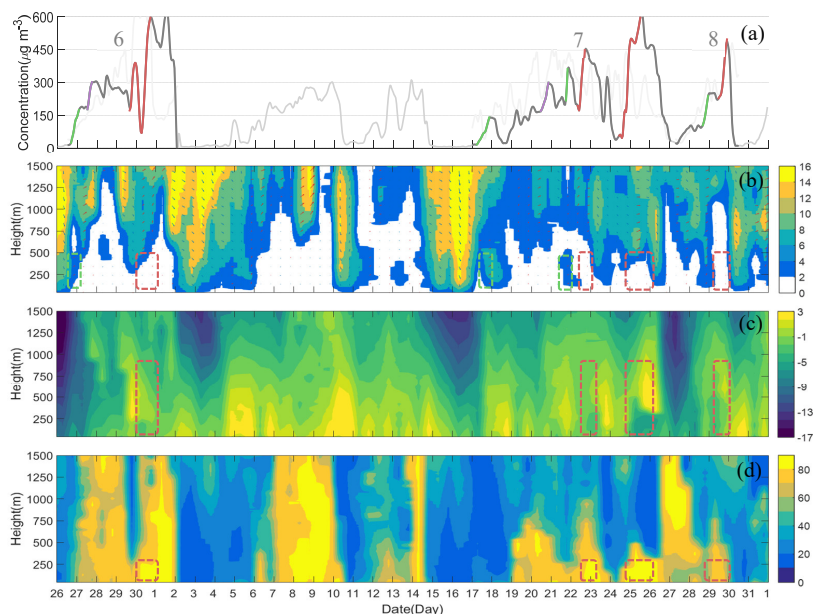
498 **February 2014. (a)PM_{2.5} mass concentration (dark gray or gray: Beijing; light gray: Baoding); (b) winds (vectors;**

499 **red vectors: southwesterly winds) and wind velocity (shadings; units: m/s); (c)temperature (shadings; units:°C);**

500 **(d)RH (shadings; units: %); (green boxes: transport explosive stages)**

501

502



503

504 **Figure 3. Temporal variations in urban mean PM_{2.5} and vertical distributions of meteorological factors in**

505 **December 2015. (a)PM_{2.5} mass concentration (dark gray or gray: Beijing; light gray: Baoding); (b) winds (vectors;**

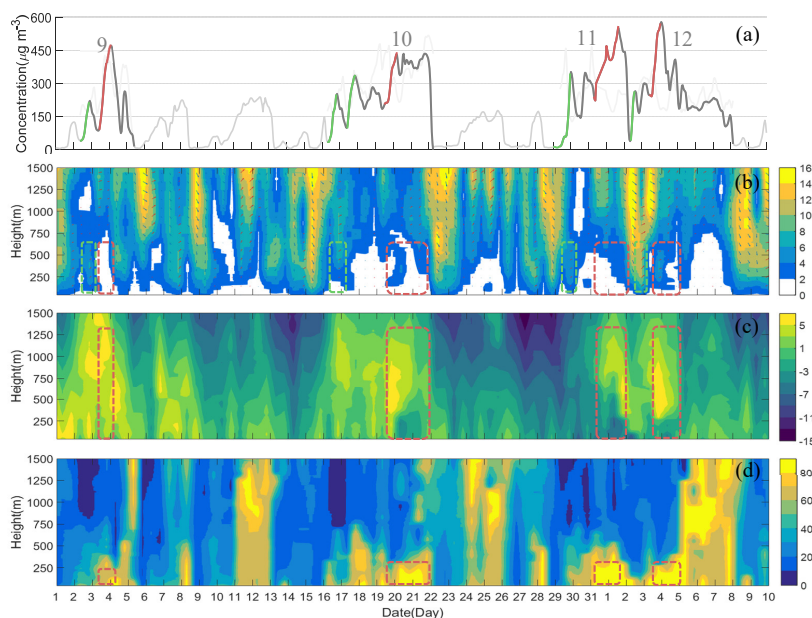
506 **red vectors: southwesterly winds) and wind velocity (shadings; units: m/s); (c)temperature (shadings; units:°C);**

507 **(d)RH (shadings; units: %); (green boxes: transport explosive stages; red boxes: cumulative explosive stages)**

508

509

510



511

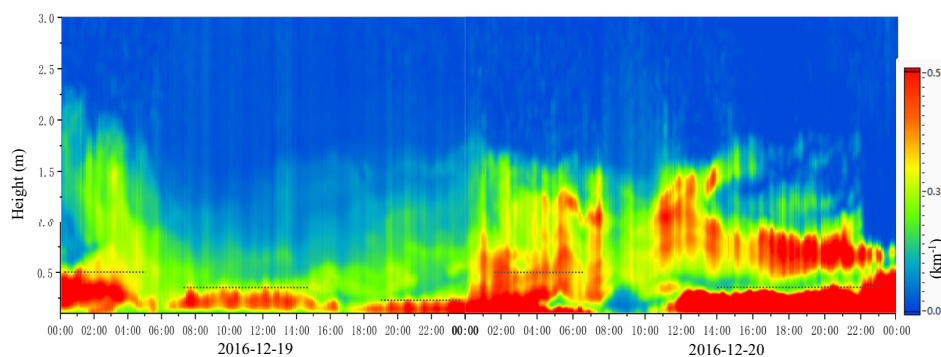
512 **Figure 4. Temporal variations in urban mean PM_{2.5} and vertical distributions of meteorological factors in**

513 **December 2016. (a)PM_{2.5} mass concentration (dark gray or gray: Beijing; light gray: Baoding); (b) winds (vectors;**

514 **red vectors: southwesterly winds) and wind velocity (shadings; units: m/s); (c)temperature (shadings; units:°C);**

515 **(d)RH (shadings; units: %); (green boxes: transport explosive stages; red boxes: cumulative explosive stages)**

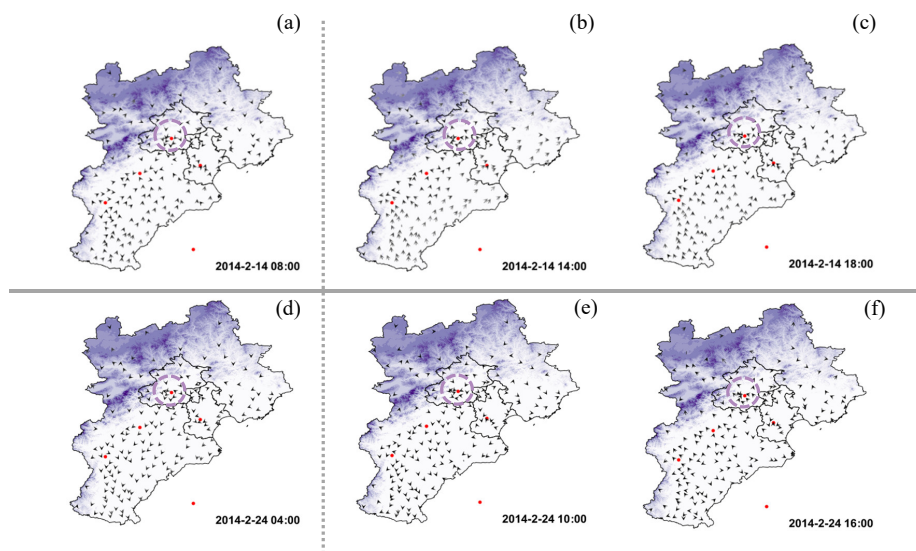
516



517

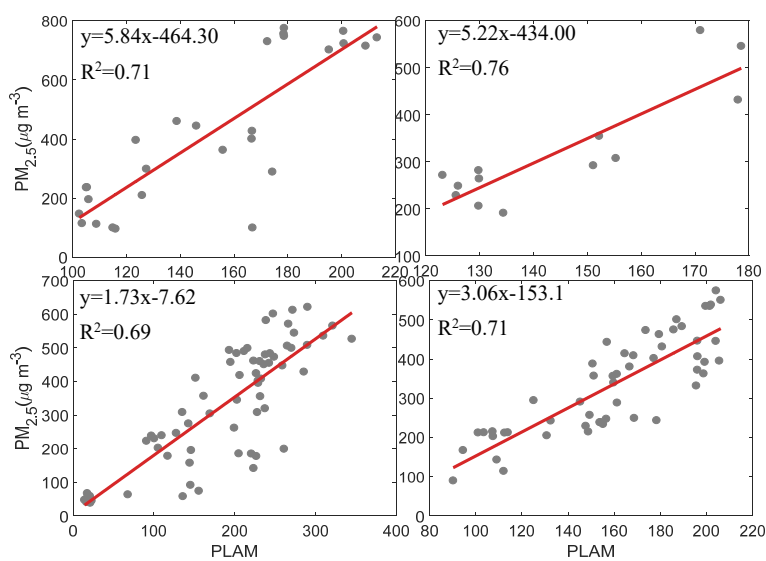
518 **Figure 5. Time series of vertical distributions of the extinction coefficient of aerosols observed in the northern**

519 **urban area of Beijing from 19 to 20 December 2016 (The dashed lines: the approximate boundary layer height)**



520

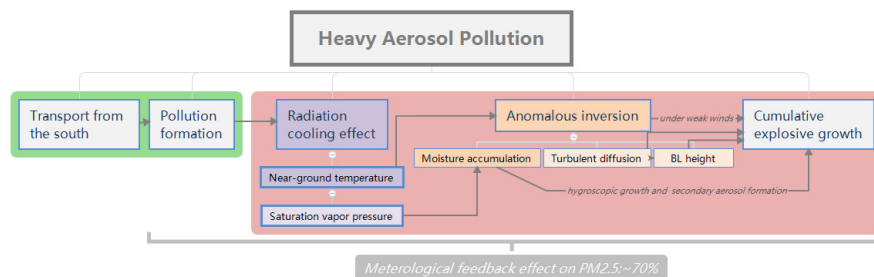
521 **Figure 6.** Surface wind distributions before (a, d) and during (b, c; d, e) two convergent explosive growth
522 processes in February 2014 on the North China Plain.



523

524 **Figure 7.** Correlation between PLAM and PM_{2.5} during the cumulative explosive growth processes in
525 January 2013 (a), February 2014 (b), December 2015 (c), and December 2016 (d) respectively.

526



527

528 **Figure 8.** A schematic figure of the formation mechanism for winter heavy pollution episodes in Beijing, which

529 consist of the transport stage (green background) and the cumulative stage (red background).